



# The Effect of Perforated Plate Geometry on Thermofluid Characteristics of Briquette Drying Oven: A 3D Computational Fluid Dynamics (CFD) Study

Samsudin Anis<sup>1,\*</sup>, Krisna Tri Romadhoni<sup>1</sup>, Deni Fajar Fitriyana<sup>1</sup>, Aldias Bahatmaka<sup>1</sup>, Hendrix Noviyanto Firmansyah<sup>1</sup>, Natalino Fonseca Da Silva Guterres<sup>2</sup>

<sup>1</sup> Department of Mechanical Engineering, Universitas Negeri Semarang, Kampus Sekaran, Gunungpati, Semarang 50229, Indonesia

<sup>2</sup> Department of Mechanical Engineering, Dili Institute of Technology, Aimeti Laran Street, Dili - Timor Leste

## ARTICLE INFO

### Article history:

Received 9 February 2024

Received in revised form 10 March 2024

Accepted 13 April 2024

Available online 30 June 2024

### Keywords:

Briquette; Drying; oven; Air distribution; CFD; ANSYS

## ABSTRACT

The process of drying briquettes in an oven is very costly due to the amount of fuel, labor, and drying time required. Furthermore, inadequate air circulation also results in an uneven and ineffective drying process for briquettes. The performance of the briquette drying oven can be improved by changing the geometry of the perforated plate in the oven to optimize the air distribution. This research process was conducted through Computational Fluid Dynamics (CFD) simulations using Ansys Fluid Flow (Fluent) software by testing three different perforated plate geometries in the oven to determine their effect on the air distribution that occurred in the oven. The research findings indicate that the temperature, velocity, pressure, and airflow pattern of the air are all considerably impacted by the incorporation of perforated plates into the first, second, and third geometries of the oven. When compared to the original geometry, the average air temperature in ovens using the first, second, and third geometries increased by 6.86%, 7.38%, and 9.15%, respectively. Average air velocity increased by 226.04%, 235.77%, and 431.60% in ovens with the first, second, and third geometries. However, the air pressure in ovens with the first, second, and third geometries decreased by 11.05%, 8.62%, and 10.66%. The use of perforated plates on the right, back, and left sides in an oven with the third geometry is the best geometry produced in this research. This happens because this oven produces the most even airflow pattern in the oven compared to other geometries. In addition, the oven with the third geometry has the highest average temperature and average air velocity, with a lower average air pressure compared to the other geometries. Consequently, drying is more effective and takes less time.

## 1. Introduction

Biomass energy sources continue to increase in terms of use and development. Biomass energy can come from plantations, agriculture, and so on. With proper processing, biomass can be utilized as charcoal and used as an alternative fuel for making briquettes [1]. Some of the raw materials for

\* Corresponding author.

E-mail address: [samsudin\\_anis@mail.unnes.ac.id](mailto:samsudin_anis@mail.unnes.ac.id) (Samsudin Anis)

briquettes from agricultural and forest materials include coconut shell, coconut shell, rice husk, sawdust waste, and many more. Indonesia as a large coconut shell producing area, coconut shell waste can be optimally utilized so that the added value of coconut shell waste increases [2]. In this regard, PT Arka Tama Indonesia is present and engaged in maximizing the utilization of widespread biomass energy, especially in the use of coconut shell biomass and firewood as the main ingredients in the processing and production of briquettes made from coconut shell charcoal.

In general, the process of making briquettes includes crushing, mixing, blending, pressing, and drying [3,4]. Drying is a mass transfer process that entails the elimination of water or another solvent through evaporation from a solid, semi-solid, or liquid substance [5–8]. As one of the producers of wood charcoal and coconut shell charcoal briquettes, PT Arka Tama Indonesia uses a wood-fired oven as a tool to dry its briquettes. However, there are several obstacles experienced in the briquette drying process, such as uneven air distribution, long drying time, high fuel and electrical energy usage, and unevenly dried briquettes in one drying process. Many briquette factories use firewood as fuel for the drying process, instead of electricity or gas to reduce production costs. Firewood is now priced at a cost that is 4, 5, and 6 times lower than diesel, gas, and electricity, respectively [9]. PT Arka Tama Indonesia's production process for coconut shell charcoal briquettes necessitates a drying duration of 3-4 days. Increasing the duration of drying results in an elevated production cost [10,11]. Furthermore, the extended drying duration will result in a reduction in the production capacity of briquettes. Drying briquettes inefficiently will increase costs and extend the production time of briquettes, so a dryer is needed that is able to dry briquettes efficiently [10,11].

The internal geometry of the oven has a significant impact on the efficiency of the oven. Different internal geometries will cause different flow patterns and flow velocities of the high temperature air entering the oven chamber, which can change the temperature distribution in the oven drying chamber resulting in different drying times [12]. According to Ngo *et al.*, [13], oven temperature distribution and heating time can be optimized by changing the geometry and position of the perforated plate in the oven. The perforated plate can affect the velocity and direction of fluid flow in the oven, so the flow pattern will also be affected. Perforated plates can enhance the evenness of temperature in the oven by decreasing the standard deviation of the average velocity of hot fluid and reducing the time required for heating [13]. Additionally, it can lead to higher hydraulic losses, causing a decrease in the average velocity and promoting the uniformity of the velocity field [14]. Furthermore, where the perforated plate is placed in the channel can change the flow, so changes need to be made to get a good agreement in terms of pressure drop and velocity distribution [15]. The results of the drying process on the oven box are influenced by the air velocity. The rate of the temperature changes and the airflow pattern within the oven box are influenced by the amount of air being supplied and the presence of orifice plates, which have a substantial impact on the flow pattern [16]. Dhanuskar *et al.*, [17] demonstrated through computational fluid dynamics (CFD) simulations that a consistent temperature distribution could be attained by altering the geometry of the oven; the perforated inlet affects both the temperature and air pressure distributions. The investigation carried out by Díaz-Ovalle *et al.*, [12] utilized computational fluid dynamics (CFD) simulations to ascertain that the configuration of oven baffle plates, including square, rectangular, and round, exerted a substantial influence on temperature distribution, pre-heating time, and oven internal temperature. The plate configuration featuring the most substantial diameter of the opening exhibits the highest level of oven performance.

Tomić *et al.*, [18] found that heat exchangers with perforated plates have the highest heat transmission when using a plate with a 0.1 porosity and 1 mm hole diameter. The research by Li *et al.*, [19] showed that the thickness of the perforated plate has a big effect on how heat moves through a flame that starts from a mixture of hydrogen and air. The apertures in the perforate plate utilized

in this investigation have a diameter of 2 mm and a thickness of 40 mm, 80 mm, and 120 mm, respectively. Their findings showed that using perforated plates with an 80 mm thickness significantly accelerated fluid flow, with the heat moving through the perforated plate being the primary cause of this acceleration. Raju *et al.*, [20] conducted research to determine the impact of perforated plate utilization in a heat exchanger on flow friction and heat transfer. Numerical research was conducted by manipulating various parameters, including plate thickness, distance between plates, diameter of holes, and arrangement of perforated plate holes, while positioned between two plates. It can be concluded from the simulations that the parameters of the perforated plate geometry have a significant impact on the hydrothermal behavior.

Numerous experimental and computational investigations have demonstrated that the utilization of perforated plates in ovens can enhance the efficiency of the drying process. However, the use of perforated plates to improve drying performance in ovens for the drying process of coconut shell charcoal briquettes has not been widely studied. Therefore, the purpose of this study is to determine the effect of perforated plate geometry on thermofluid characteristics, which include temperature distribution, velocity, airflow pattern, and air pressure in the briquette drying oven. This study is necessary due to the significant drawbacks encountered during the briquette drying process, including prolonged drying duration, higher labor expenses, and excessive fuel use. The design of the briquette drying oven in this study is based on the existing biomass-fueled coconut shell charcoal briquette drying oven owned by PT Arka Tama Indonesia, which is located in Rawamerta District, Karawang Regency, West Java, Indonesia. The present study utilized ANSYS Fluent 2022 R1 to conduct computational fluid dynamics (CFD) simulations. CFD simulation offers an affordable, efficient, and cost-effective alternative to manual analysis in manufacturing processes, such as drying briquettes using biomass-fueled ovens, enhancing efficiency, reducing emissions, and improving product quality [21,22].

## 2. Methodology

### 2.1 Simulation Data

Before the simulation process, it was necessary to take experimental data on the tool in the form of geometry and dimensions of the oven, temperature in the combustion chamber as a heat source, and temperature in the oven room to enter the temperature value in the setup process later. The Arka Tama factory's briquette drying oven was built using iron plate for the frame, body, and furnace, and stainless steel for the perforate plate (Table 1).

**Table 1**  
Oven materials and sizes

Parts	Materials	Size	Thickness (mm)
Body	Iron plate	3×4×2 m	1.5
Heat insulation	Glasswool	-	50
Furnace	Iron plate	50×50×70 mm	3
Large inlet pipe	Iron pipe	8 inch	15
Small inlet pipe	Iron pipe	4 inch	10
Perforated plate	Stainless	∅ 20 mm	1.5

Dimensional measurements were made using a meter and obtained dimensions of 3 m × 4 m × 2 m (length × width × height) and had two doors on the front side. The oven body was made of iron plate coated with glasswool (heat absorbers), then for the combustion furnace made of iron and iron pipes in the inlet channel with a diameter of 4 inches and 8 inches with a thickness of 15 mm. The

biomass oven operated using firewood fuel. The temperature was measured using a thermometer that had been installed in the oven to determine the temperature in the oven during the briquette drying process. From these observations, the temperature of the combustion chamber (heat source) was 200°C, while the temperature inside the drying chamber near the front wall was 90°C. According to research by Araújo *et al.*, [23], a sufficiently high airflow velocity at the inlet will affect the drying rate where it can change the air distribution and shorten the drying time. Then from the simulation results, a velocity of 2 m/s can provide the best temperature distribution [24].

## 2.2 Oven Geometry Design and Meshing Process

The design of the biomass-fueled briquette drying oven was made using Autodesk Inventor Professional 2022 Students Version software which was then exported in .STP format and inputted into ANSYS Fluid Flow (Fluent) software for further simulation (Figure 1).

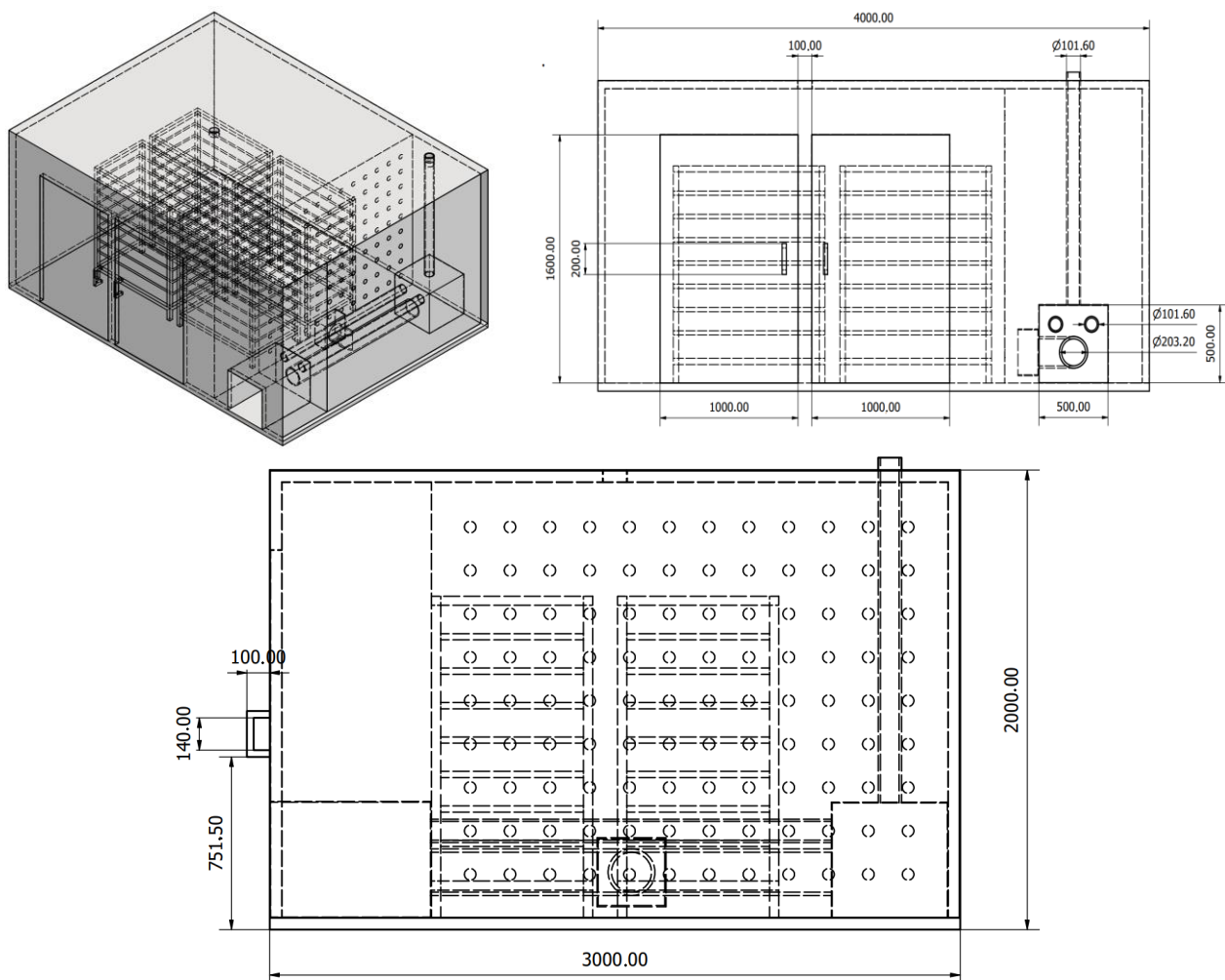


**Fig. 1.** Briquette drying oven design (mm)

The design of the oven that had been made using Autodesk Inventor Professional 2022 software was then entered into ANSYS Fluid Flow (Fluent) 2022 R1 software for further meshing and simulation processes.

In the mesh step, mesh refinement can be done if needed in several ways such as changing the element size, adding mesh sizing and mesh method to the selected oven part, and by setting the

minimum curvature size. The quality of the meshing results was seen with the skewness mesh quality matrix method to determine the quality of the elements formed from the meshing process. In addition, an independent mesh study was conducted with different element sizes and number of elements and the skewness quality was compared. If the mesh quality had shown good results and there was no significant change in quality, the mesh variation can be selected for validation. The meshing validation process was done by comparing the simulated data using several mesh variations using a mesh with acceptable skewness quality. The named selection process was carried out on certain parts of the oven design according to simulation needs so that it would facilitate the determination of boundary conditions in the setup process later. The named selection process was carried out on several parts such as the cross section of the air inlet, fluids, and outlet. The air inlet cross section had a size of 50 × 50 cm or an area of 0.25 m<sup>2</sup>.

### 2.3 Simulation Setup

The setup process was part of setting or determining the conditions of the model to be simulated. This process was carried out to define the process, parameters, and enter engineering data so that the simulation run according to the desired conditions. In CFD simulation, setup was done to define how the simulation will be run. Based on research by Edirisinghe *et al.*, [25], the treatment in the setup is organized with the following details:

- i. Time is set to steady because the simulation is done to see the temperature distribution that is not limited to a certain time.
- ii. The solver type is pressure based.
- iii. Gravity parameter is enabled, and the value is set to -9.81 m/s<sup>2</sup>.
- iv. Energy is set on to facilitate heat transfer and temperature changes throughout the computational domain.
- v. The walls and other parts of the oven are set to radiant heat transfer mode. Meanwhile, the perforated plate is set to adiabatic mode.

According to Park *et al.*, [26], radiant heat transfer is set using the Discrete Ordinates (DO) model which is better at solving the radiant heat transfer equation over several angles related to the airflow direction. Then, turbulent modelling uses the k-omega SST model because the model combines the advantages of the k-Epsilon model which is suitable for free stream flow distance from the wall and the advantages of the k-omega standard model, which is suitable for flow near the wall area, so that the k-omega SST model is more flexible according to the distance of fluid flow from the wall. The setup is opened by activating double precision, then in the boundary conditions, the inlet is set as a mass flow inlet while the outlet is set as a pressure outlet with a gage pressure value of 0 (zero) or equal to atmospheric pressure. The absolute pressure value at the inlet cross section is determined by the density value ( $\rho$ ) of air at sea level through the following equation.

$$P = \rho RT \tag{1}$$

So that the absolute pressure value at (inlet) with a temperature 200°C (473.15°K) is obtained through the following calculation.

$$P = 1.225 \frac{kg}{m^3} \times 286.9 \text{ J/kg.K} \times 473.15^\circ K$$

$$P = 166289.75 \text{ Pa}$$

With an absolute pressure value of 166289.75 Pascal, the gauge pressure value at the inlet is determined by reducing the absolute pressure value to the atmospheric pressure value.

$$P_g = P - P_o \quad (2)$$

$$P_g = 166289.75 \text{ Pa} - 101330 \text{ Pa}$$

$$P_g = 64959.75 \text{ Pa}$$

so that the initial gauge pressure value at the inlet is set at 64959.75 Pascal. Then, the mass flow rate value at the inlet is set according to the following calculation.

$$\dot{m} = \rho VA \quad (3)$$

$$\dot{m} = 1.225 \frac{\text{kg}}{\text{m}^3} \times 2 \frac{\text{m}}{\text{s}} \times 0.25 \text{ m}^2$$

$$\dot{m} = 0.6125 \frac{\text{kg}}{\text{s}}$$

So, that the mass flow rate at the inlet cross section is set to a value of 0.6125 kg/s with an inlet air velocity of 2 m/s.

#### 2.4 Geometry Variation of Perforated Plate Briquette Drying Oven

In this study, three variations of the first, second, and third perforated plate geometry were made with different plate positions and hole positions as shown in Figure 2.

The first geometry variation was modeled using one side of a 1.5 mm thick perforated plate on the right side of the drying chamber with a total of 108 holes and a diameter of 50 mm. The second geometry variation was modeled using two 1.5 mm thick perforated plates on the right and back of the drying chamber with a total of 108 holes and a diameter of 50 mm divided into 54 holes per side (right side and back). While the third geometry variation was modeled using three 1.5 mm thick perforated plates on the right, back, and left side of the drying chamber with a total of 108 holes and a diameter of 50 mm divided into 36 holes per side (right, back, and left side).

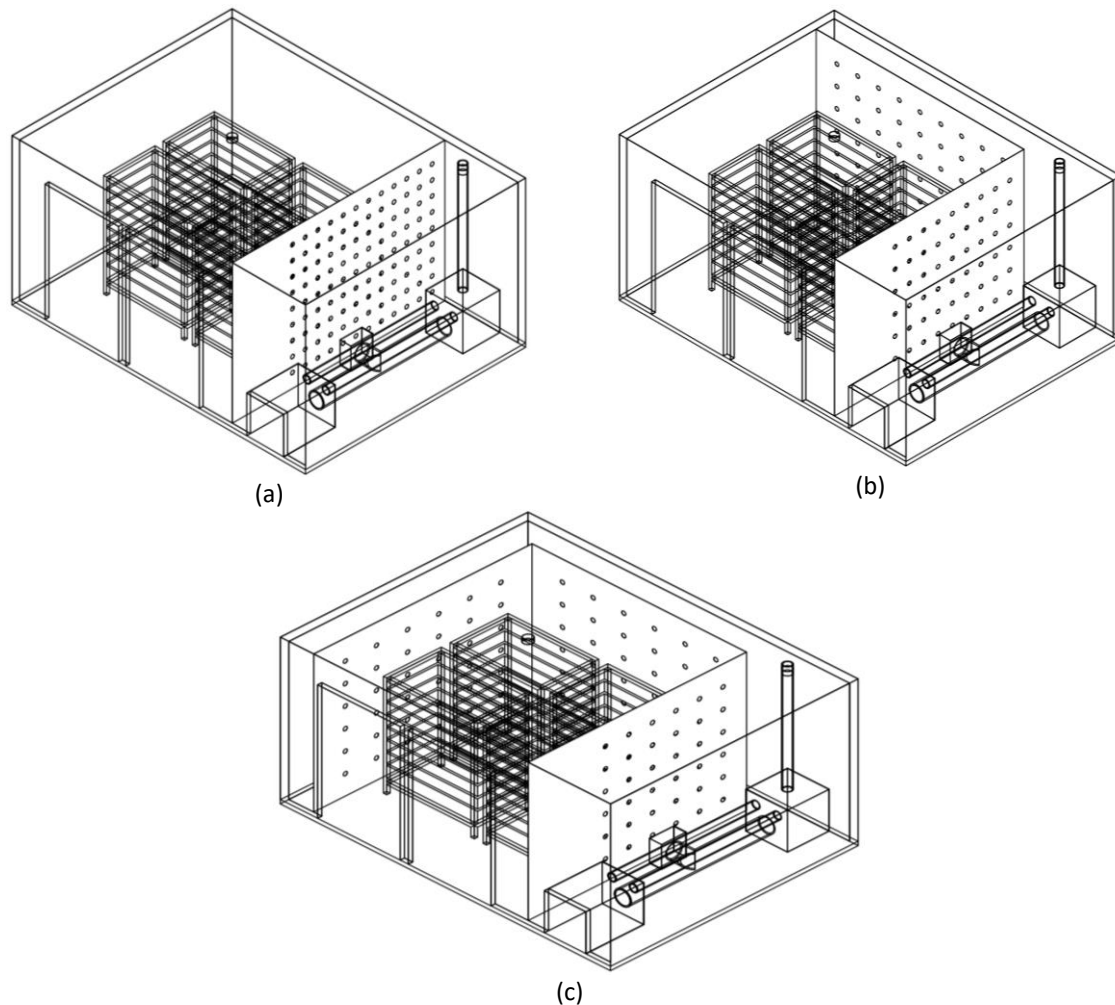


**Fig. 2.** Geometry of (a) first, (b) second, and (c) third perforated plates

### 2.5 Data Collection Technique

The data collection process was carried out by taking measurements and simulations to collect the required data. After collecting all of the data, it was gathered and evaluated to complete the study's objectives. Direct measurements were taken at the oven to collect air temperature data at two points, namely in the wood biomass combustion furnace room and in the briquette drying room which was located close to the front wall of the oven. Data regarding the measurement of the distribution of air temperature, air velocity, and air gauge pressure in the oven was determined by adding eight measurement points that served as measurement positions for air temperature, air velocity, and air gauge pressure to be analyzed and compared for distribution (Figure 3). The data that had been obtained and analyzed was then presented in the form of tables, figures, and descriptions in the form of explanations to explain the simulation results data.

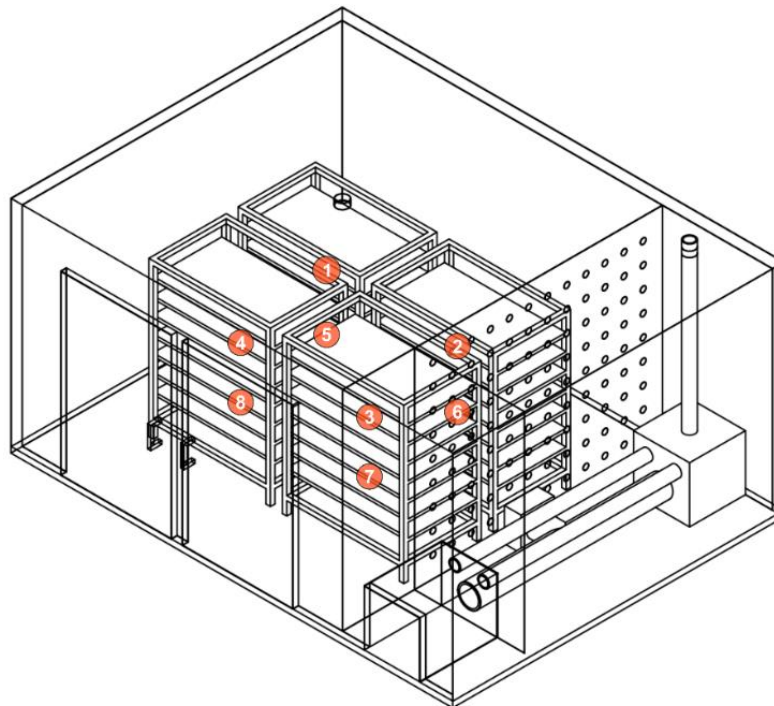


**Fig. 3.** Eight measurement points for temperature, velocity, and pressure of air

### 3. Results and Discussion

#### 3.1 Mesh Independent Study

A mesh independent study is conducted to determine the meshing with the right settings and obtain the optimal mesh size and solution [27]. By performing variations such as element size, mesh quality can be divided into fine mesh and coarse mesh or into several other parts as needed.

If the difference in simulation results between mesh variations is small, then the simulation can be carried out using a mesh with optimal quality for the computing power and time reached by the computer.

From the Table 2, nine mesh experiments were conducted using different element sizes with their respective qualities. However, a small element size with a larger number will make the simulation process heavier on the computer, so a larger element size with a smaller number of elements can be selected to reduce the simulation load.

**Table 2**  
 Independent study mesh result data

<i>Element size (mm)</i>	<i>Curvature min size (mm)</i>	Number of elements	<i>Skewness average</i>
300	25	552972	0.28615
280	24	591133	0.28567
260	23	637623	0.28206
240	22	688007	0.27806
220	21	750229	0.27435
200	20	832774	0.27280
180	19	933843	0.26764
160	18	1078033	0.26410
140	17	1286464	0.26023



### 3.2 Mesh Validation

Figure 4 depicts the measurement points conducted directly in this study. Point 1 depicts the wood biomass combustion chamber or furnace within the oven. Point 2 illustrates the oven area specifically designated for dry briquettes. The mesh validation process in this study employs the original oven geometry utilized by PT Arka Tama Indonesia. The original oven utilizes a perforated plate positioned on the right side of the drying chamber, with a hole diameter of 20 mm.

Mesh validation is performed by assessing the number of meshes derived from the findings of the previously conducted mesh-independent investigation.

Mesh validation is conducted to verify that the mesh settings and techniques employed are suitable and produce minimal error compared to the experimental measurement data. Figure 5 illustrates a comparison of temperature values obtained through direct measurement with the findings obtained through simulation. The temperature in the oven room is measured to be 90°C. The simulation, which closely matches this temperature, is achieved utilizing 832774 elements and results in a temperature of 87.161°C (Figure 5(a)). The study's findings indicate that the temperature measured in the furnace oven is 200°C. The simulation results indicate that when the number of elements of 750229, 832774, 933843, and 1078033, the temperatures obtained are approximately 200 °C (Figure 5(b)). According to the results of this study, the number of elements 832774 provides the lowest average error when compared to the other numbers of elements. The average error resulting from the utilization of the number of elements, 832774, is 1.577%. Furthermore, the simulation process will use a mesh with a size of 200 mm and a number of elements of 832774.

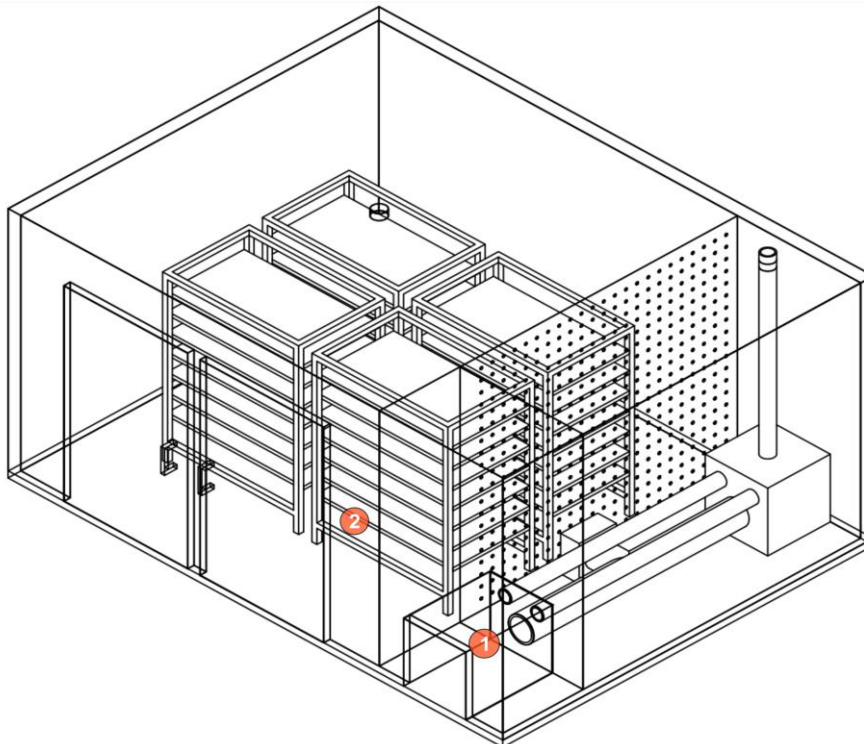


**Fig. 4.** Position of two temperature measurement points for validation of mesh results

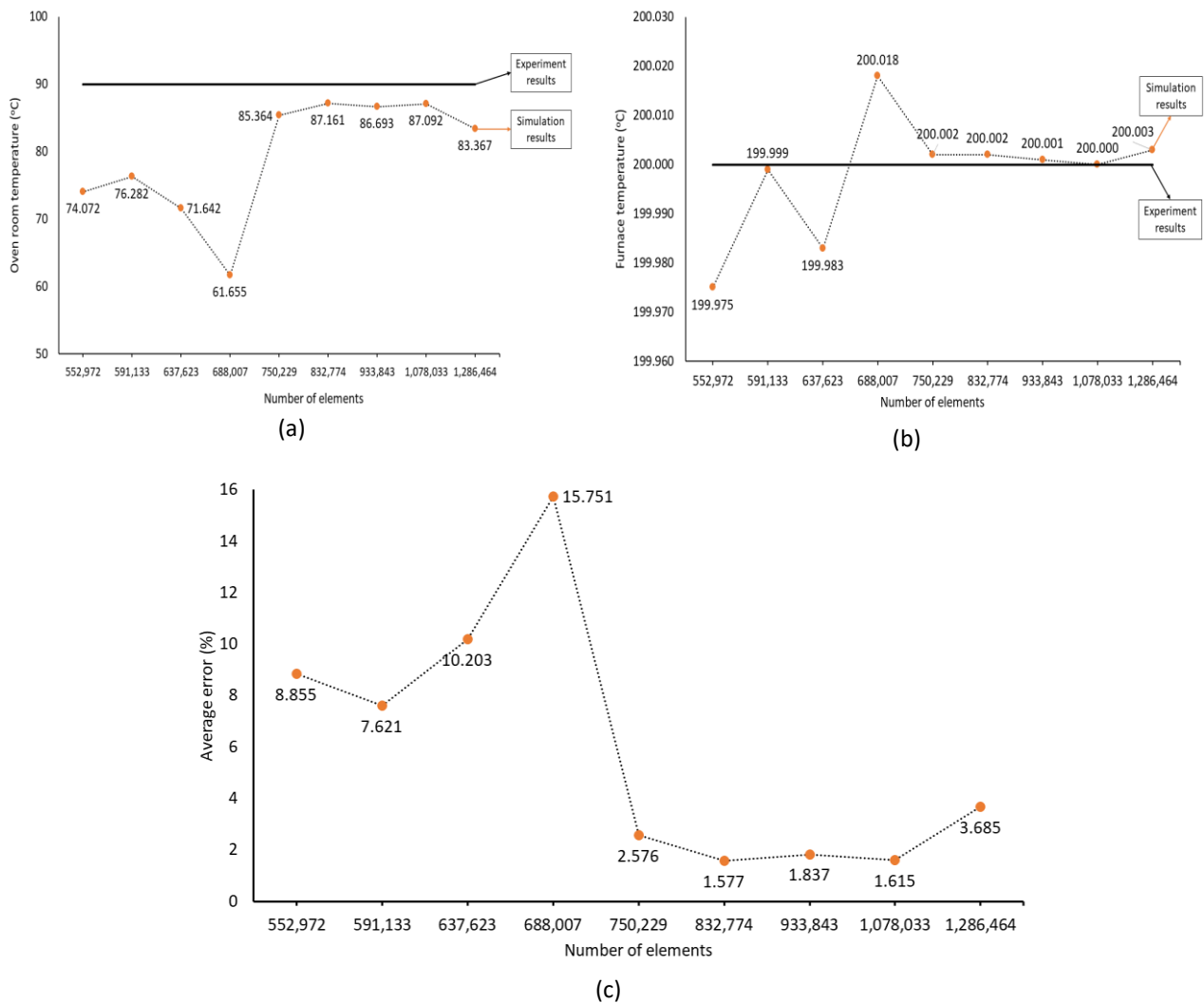


**Fig. 5.** Mesh validation between experiment and CFD simulation results (a) oven room, (b) furnace, (c) average error

The name selection process in the boundaries is shown in Figure 6. The form of giving names is carried out on certain parts of the oven design according to the needs of the simulation. In order to determine boundary conditions in the setup process later, the named selection process is carried out in several parts, such as the air inlet cross section (inlet), fluids, and outlet.

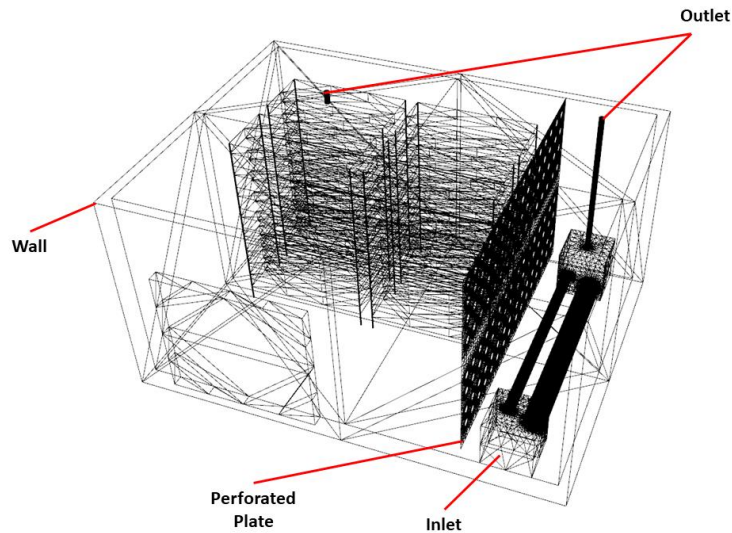


**Fig. 6.** The name selection process in the boundaries

### 3.3 Air Temperature Analysis

Figure 7 shows the contours of the air temperature distribution that occurred inside the oven chamber using the original oven geometry and the three perforated plate geometry variations.

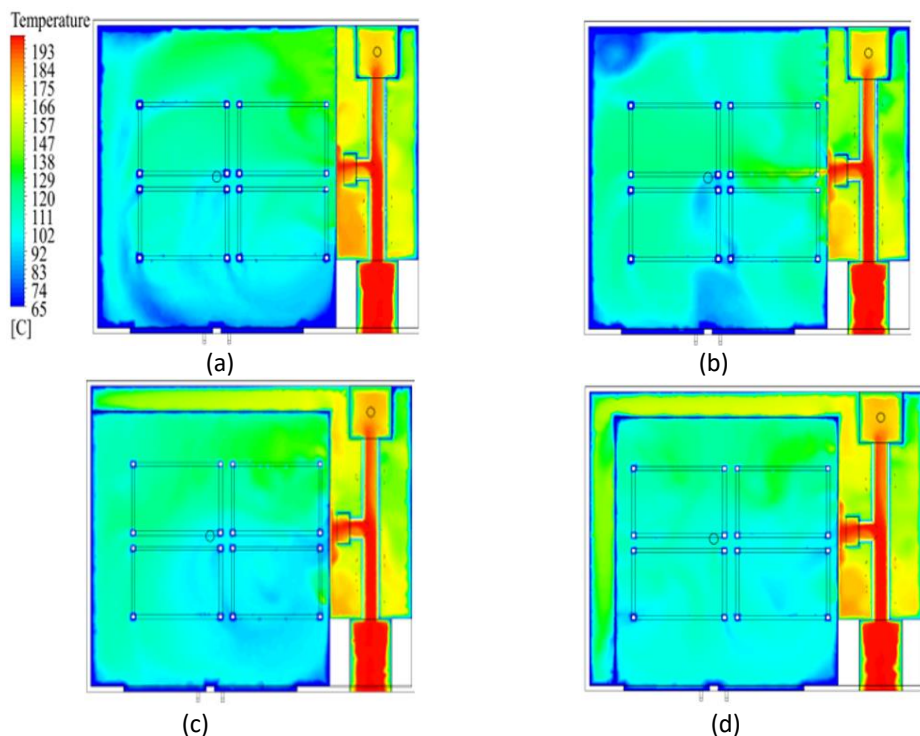


**Fig. 7.** Air temperature distribution contours at the bottom of the oven with (a) original geometry, (b) 1st geometry, (c) 2nd geometry, and (d) 3rd geometry viewed from the top side of the oven

The simulation results show a difference in air temperature distribution in the oven. In all oven models, the temperature distribution shows that air close to the perforated plate produces higher temperatures. While the air further away from the perforated plate has a lower temperature. The perforated plate rapidly absorbs heat from the heating element and subsequently emits it into the

surrounding air through radiation. Consequently, the air close to the perforated plate exhibits a raised temperature.

Figure 8 displays the air temperature at eight designated measurement points. The investigation findings indicate that the original oven recorded a minimum temperature of 62.483°C, a maximum temperature of 84.859°C, and an average temperature of 74.093°C. The first geometry oven generated the maximum temperature recorded, which was 91.275°C. In the first geometry oven, the minimum and average temperatures recorded were 62.518°C and 79.172°C, respectively. When perforated plates were used in the first geometry oven, the maximum, average, and minimum temperatures all increased in comparison to the original oven. The highest temperature, average temperature, and minimum temperature in the first geometry oven all increased by 7.56%, 6.86%, and 0.06%, respectively, according to the findings of this study.

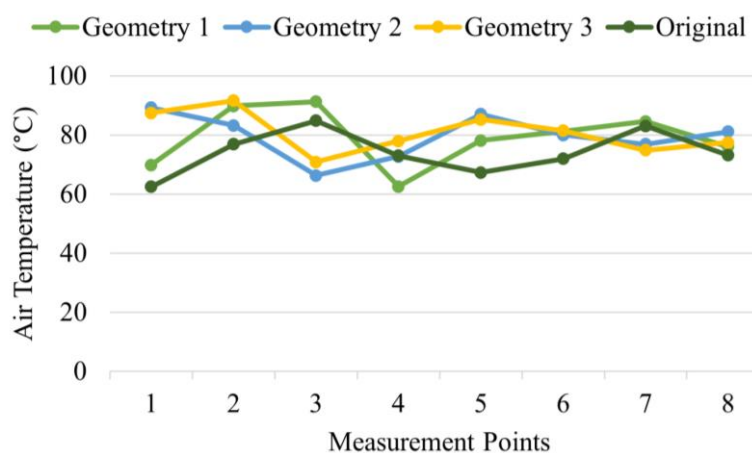


Fig. 8. Graph of air temperature at eight measuring points

The highest temperature recorded in the second geometry oven was 89.281°C. The second geometry oven obtained minimum and average temperatures of 66.251°C and 79.562°C, respectively. When perforated plates were used in the second geometry oven, the maximum, average, and minimum temperatures all increased compared to the original oven. Maximum, average, and minimum temperatures in the second geometry oven rose by 5.21%, 7.36%, and 6.03%, respectively, according to the results of this study. Furthermore, in the third geometry oven, the maximum temperature recorded was 91.607°C. The minimum and average temperatures recorded in the third geometry oven were 70.893°C and 80.869°C, respectively. Perforated plates in the third geometry oven increased the maximum, average, and minimum temperatures compared to the original oven. The findings in this study show that the maximum temperature, average temperature, and minimum temperature in the third geometry oven increased by 7.95%, 9.15%, and 13.46%, respectively. The results of this study show that the use of perforated plates has a significant contribution to increasing the average temperature in the oven. In the original, first geometry, second geometry, and third geometry ovens, the average temperature inside the oven was 74.093°C, 79.173°C, 79.562°C, and 80.869°C, respectively. The oven with the third geometry had the highest average temperature. According to Horuz *et al.*, [28], higher air temperature in the drying equipment will accelerate the heat transfer process in the dried material, so that the material will dry faster. Higher air temperatures lead to an accelerated rate of water evaporation from the product. As a consequence, the drying process is accelerated [29–31].

In addition, the use of perforated plates makes a significant contribution to the temperature difference in the oven. This temperature difference is calculated based on the difference between the maximum and minimum temperatures in the oven. The findings in this study show that the

temperature differences in the original, first geometry, second geometry, and third geometry ovens are 22.376°C, 28.757°C, 23.030°C, and 20.714°C, respectively. A decreased temperature difference means a more homogeneous dispersion of heat, whereas an increased temperature difference indicates an uneven dispersion of heat. Therefore, the oven with the third geometry exhibits superior heat distribution compared to other models. This occurs because the oven with the third geometry has the smallest temperature difference.

According to Smolka *et al.*, [32], the oven's heat source must be carefully designed to achieve the desired temperature distribution. To ensure the highest quality of the device, it is crucial to achieve a high degree of temperature uniformity by making the temperature as consistent and even as possible. The material experiences ideal drying conditions from the beginning due to the homogeneous distribution of heat. Every part of the material is evenly exposed to sufficient heat at the same time, reducing the total drying duration. This obviates the necessity for certain regions to endure waiting for heat to penetrate them, leading to the expedited and more effective elimination of moisture.

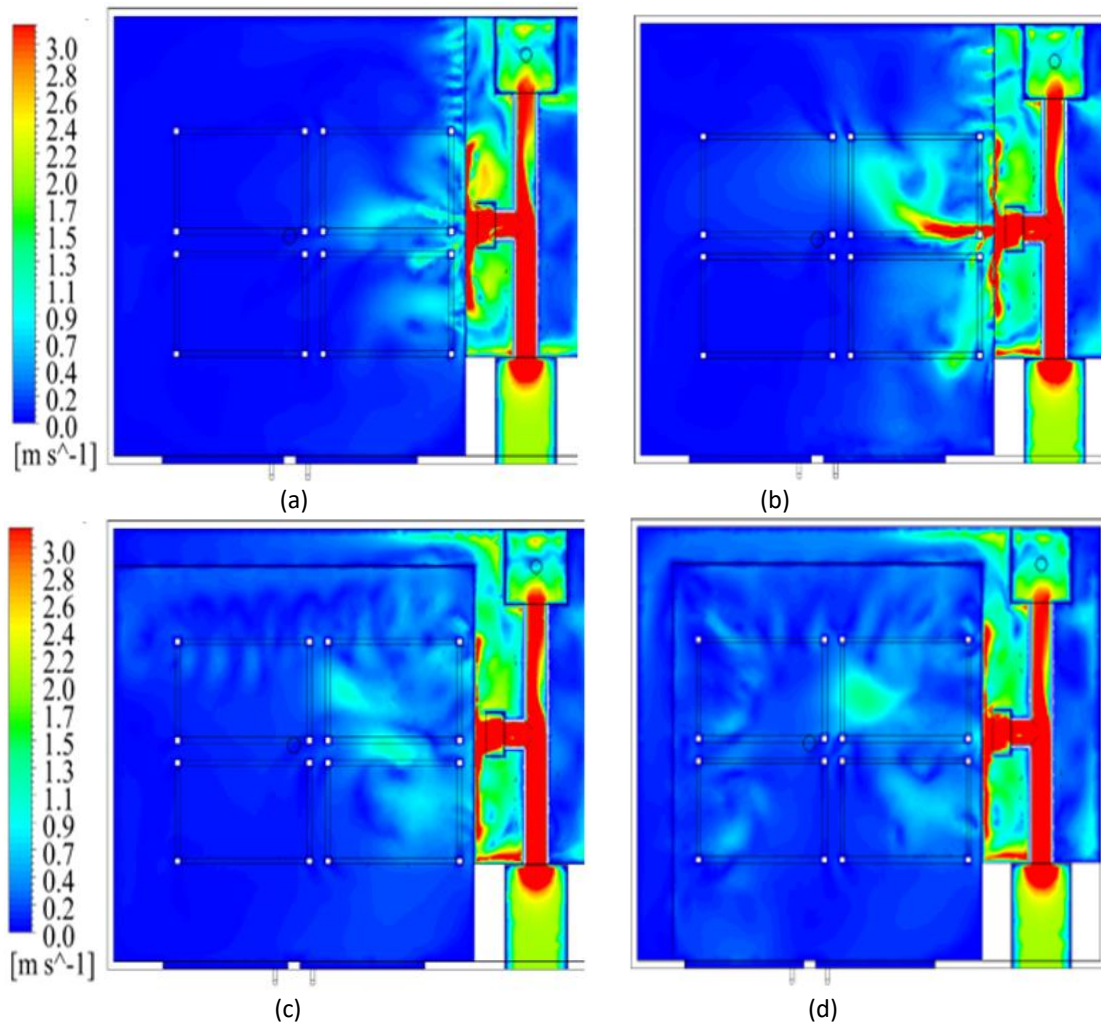
### 3.4 Air Velocity Analysis

Figure 9 shows the contours of the air velocity distribution inside the oven. The simulation findings indicate differences in air velocity distribution within the oven. The velocity distribution in all oven models indicates that the air close to the perforated plate exhibits higher velocities.

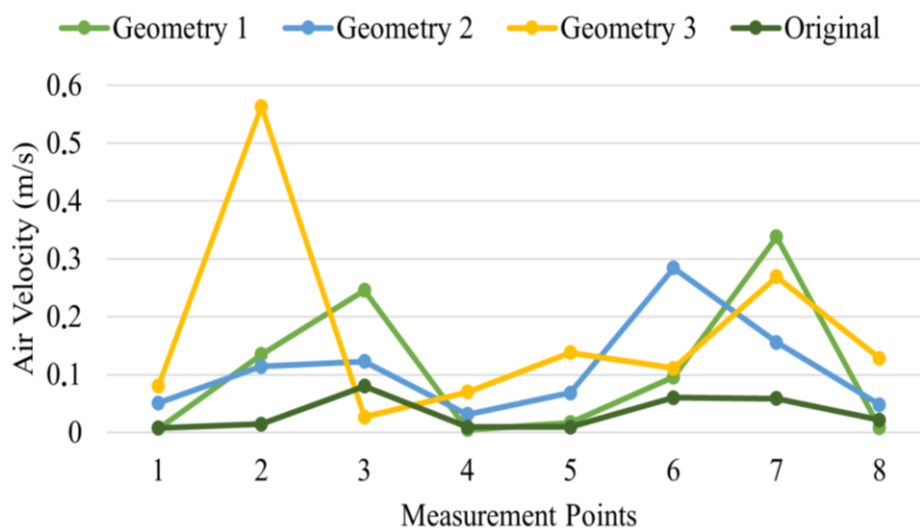
The air located at a greater distance from the perforated plate has a lower velocity. The highest air velocities in the original, first geometry, second geometry, and third geometry ovens were found at measurement points 3, 7, 6, and 2, respectively. Perforated plates can induce flow rectification, wherein the incoming airflow is redirected and compelled to pass through the holes or apertures in the plates. The diversion might induce turbulence and augment the air velocity that traverses the perforations [33].

Figure 10 illustrates the air velocity at the eight designated measurement points. The investigation revealed that the original oven had a minimum air velocity of 0.0078 m/s, a maximum air velocity of 0.0798 m/s, and an average air velocity of 0.0326 m/s. The first geometry oven achieved a maximum air velocity of 0.3380 m/s, which is the highest recorded value. The first geometry oven exhibited air velocities of 0.0046 m/s and 0.1063 m/s as the minimum and average values, respectively. When a perforated plate is introduced into an oven with the initial geometry, the maximum and average air velocities experience a significant rise of 323.56% and 226.04%, respectively, in comparison to the original oven. In contrast, the oven with the first geometry experienced a 41.03% decrease in velocity compared to the minimum velocity in the original oven. In addition, the maximum velocity measured in the second geometry oven was 0.2842 m/s. The second geometry oven achieved a minimum velocity of 0.0311 m/s and an average velocity of 0.1095 m/s. Using perforated plates in the second oven geometry resulted in an overall increase in the maximum, average, and minimum velocities compared to the original oven.





**Fig. 9.** Air velocity distribution contours at the bottom of the oven with (a) original geometry, (b) 1st geometry, (c) 2nd geometry, and (d) 3rd geometry viewed from the top side of the oven



**Fig. 10.** Graph of air velocity at eight measuring points

The study found that the maximum, average, and minimum velocities in the second geometry oven increased by 256.14%, 235.77%, and 298.72% respectively. Furthermore, the highest velocity

measured in the third geometry oven was 0.5633 m/s. The minimum and average velocities measured in the third geometry oven were 0.0267 m/s and 0.1733 m/s, respectively. The use of perforated plates in the third geometry oven resulted in higher maximum, average, and minimum velocities as compared to the original oven. The results of this investigation indicate that the maximum velocity, average velocity, and minimum velocity in the third geometry oven experienced a significant rise of 605.89%, 431.60%, and 242.31%, respectively.

The results of this study show that the use of perforated plates has a significant contribution to increasing the average velocity in the oven. In the original, first geometry, second geometry, and third geometry ovens, the average air velocity inside the oven was 0.0326 m/s, 0.1063 m/s, 0.1095 m/s, and 0.1733 m/s, respectively.

The oven with the third geometry had the highest average air velocity. Increased air velocity enhances the process of water vapour evaporation from the material's surface. Increased air velocity enhances moisture transport, leading to more effective evaporation and accelerated drying. Furthermore, increasing the air velocity improves the rate of mass transfer between the air and the substance being dried. This enhances the surface area of contact between the air and the substance, facilitating a more effective extraction of moisture [34]. The slow evaporation of moisture from the material to the environment leads to a longer drying time [35]. According to Araújo *et al.*, [23], The speed of the air flowing in the dryer will affect the drying process of the material, faster flowing air will shorten the drying time. Air that does not flow properly will increase the water vapor content around the dried material so that the drying time is slower. The results obtained from this study align with those reported in the study by Erdiwansyah *et al.*, [36]. According to their findings, the use of perforated plates could improve air velocity in the fluidized-bed combustion chamber. Modifying the geometry of the perforated plate may lead to slightly higher air velocities.

### 3.5 Air Pressure Analysis

Figure 11 shows the contours of the air gauge pressure distribution occurring inside the oven chamber of the briquette dryer when viewed from the top viewpoint of the oven. The results of this study show that the air pressure distribution in the oven varies with the use of a perforated plate. The air pressure in the original oven is higher than in other oven models.

The type of fluid and pressure that flows will affect the heat transfer that occurs in a device [37]. High air pressure can restrict airflow inside the oven, thereby reducing the effectiveness of heat and moisture transfer. This can cause the drying of the product to occur unevenly and take a long time [38]. Drying is the process of extracting moisture from the product.

Increased pressure in the air can influence the kinetics of moisture extraction, resulting in changes in the evaporation rate. This could lead to prolonged drying durations as the moisture extraction process is decelerated [39].

The air pressure at the eight designated measurement points is shown in Figure 12. The research findings indicate that the maximum air pressure recorded in the ovens with the original, first geometry, second geometry, and third geometry was 2267.08 Pa, 2016.54 Pa, 2071.75 Pa, and 2025.93 Pa, respectively. The minimum air pressure in the original, first, second, and third geometry ovens is 2267.01 Pa, 2016.20 Pa, 2071.41 Pa, and 2025.27 Pa, respectively. The average air pressure in the original, first, second, and third geometry ovens is 2267.05 Pa, 2016.47 Pa, 2071.64 Pa, and 2025.40 Pa, respectively. The results of this research show that all oven models produce air pressure inside the oven that has almost the same value at all measurement points. The original oven has the highest air pressure compared to other ovens. The use of a perforated plate with a certain geometry in this research has a significant effect on reducing the air pressure in the oven. Ovens with the

second geometry have higher air pressure than ovens with the first and third geometries. Meanwhile, the air pressure in ovens with the first and third geometries has a low value and is not significantly different. Furthermore, according to Li *et al.*, [40], pressure and temperature are two important parameters in thermodynamics and affect each other. The lower the fluid temperature, the higher the air pressure and density.

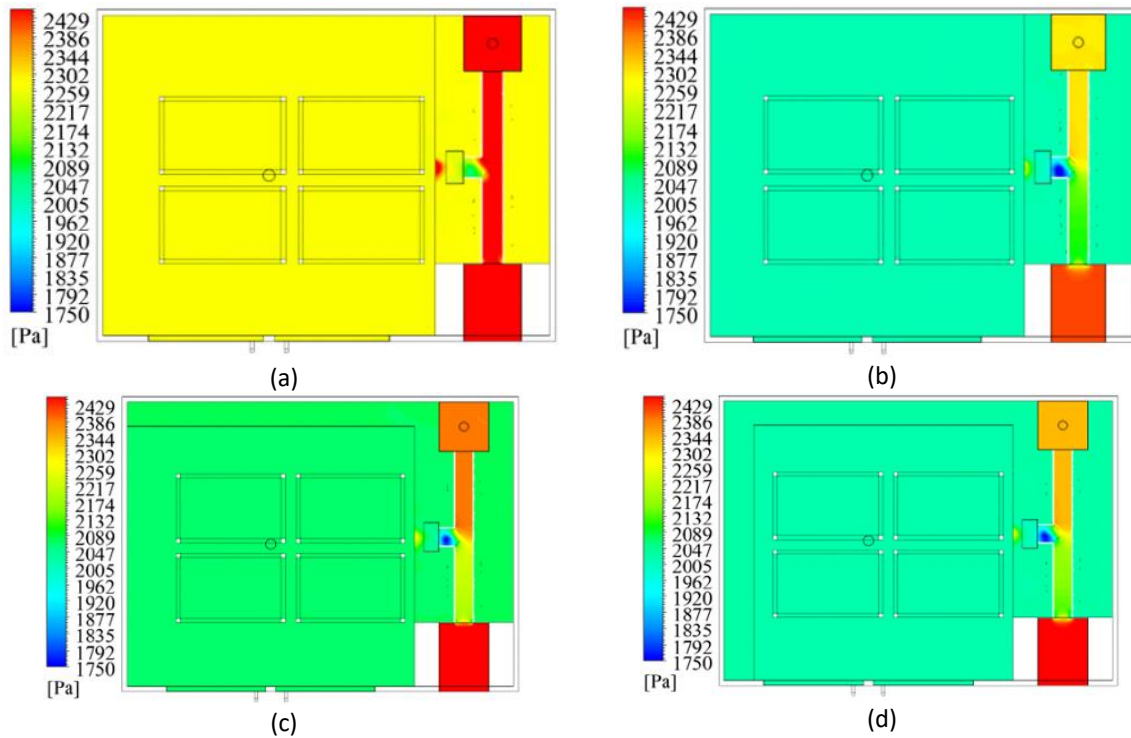


**Fig. 11.** Air pressure contours of the oven with (a) 1st geometry, (b) 2nd geometry, and (c) 3rd geometry

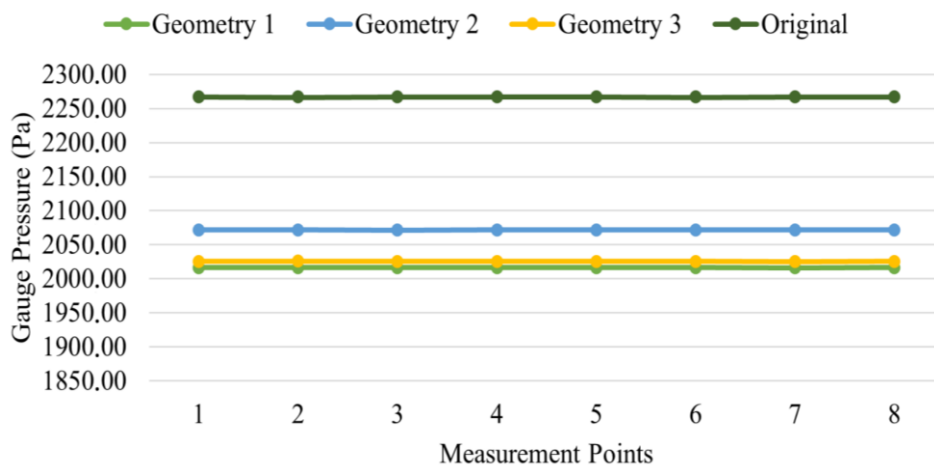


**Fig. 12.** Graph of air gauge pressure at eight measuring points

Temperature greatly affects the drying of materials which is affected by the air pressure. Decreasing air pressure enhances the capacity of the air to remove moisture from the material during the drying process. Decreased air pressure corresponds to lower air density, facilitating the collection and removal of moisture from the substance [41]. Elevated air pressure leads to an increase in air humidity [42–44], resulting in a reduction in the air's capacity to retain moisture. Consequently, this



impedes the drying process of the material. Furthermore, a decreased air pressure within the oven results in a corresponding decrease in air humidity. This can accelerate the drying process, as air with low humidity has a reduced ability to retain water vapor. Consequently, the extraction of water from the desiccated substance can be expedited [45,46].

According to another references, elevated air pressure can impede the process of water vapor evaporation from dehydrated goods. High air pressure reduces the rate at which water vapor molecules are released from the surface of a material, resulting in slower drying and prolonging the drying process [47].

Moreover, excessive air pressure might impede moisture movement and decrease the convective heat transfer coefficient. This additionally adds to decelerating the rate at which drying occurs and impacts the operation's overall effectiveness [48].

### 3.6 Airflow Pattern Analysis

The resultant airflow pattern is depicted in Figure 13. The findings of this study demonstrate that the utilization of perforated plates has a notable impact on the flow patterns of air. The major airflow pattern in all modern oven designs is through the perforated plate holes. According to Díaz-Ovalle *et al.*, [12], the airflow pattern within the oven room will impact the distribution and velocity of temperature. The presence of localized airflow indicates an uneven distribution of temperature and air velocity inside the oven room. Therefore, to ensure that the drying process is more effective and efficient, an even airflow pattern that is directed in the same direction as the temperature distribution and air velocity is required. Luo *et al.*, [49] found that conventional electric ovens have uneven heat circulation, which is concentrated at the oven's edges. This results in the cooked meal having a rough and charred exterior while the inside remains uncooked. To solve this issue, it is necessary to maintain a consistent temperature in the oven while ensuring that the air circulation within the oven remains steady. The purpose of having a uniform airflow in the oven is to maintain a consistent temperature [49].

The results of this investigation indicate that the airflow pattern in the first geometry oven and the original geometry is more concentrated on the right side. This region serves as the air entry route from the furnace via the perforated plate. The airflow pattern is more uniform in the oven utilizing the second geometry compared to the ovens utilizing the first and original geometries. This occurs due to the utilization of perforated plates situated on the rear and right sides of the oven. Compared to other oven models, the airflow pattern in the third geometry oven is superior. This occurs due to the airflow passing through the perforated plates on the left, right, and posterior surfaces. As a result, air circulation becomes more uniform. By incorporating perforated plates on the right, rear, and left sides, the oven with the third geometry achieves an optimal airflow pattern within the drying chamber for coconut shell charcoal briquettes, ensuring the most uniform distribution of air.

The findings of this investigation align with those of a study carried out by Ngo *et al.*, [13]. Their research demonstrates that the utilization of perforated plates can substantially increase temperature uniformity and decrease oven heating time, in addition to playing a crucial role in air distribution within the oven. The standard deviations obtained for cases without perforated plates, using perforated plates at the back and front are 2.34 m/s, 0.45 m/s, and 0.31 m/s, respectively. As the standard deviation decreases, the temperature and fluid velocity distribution within the oven become more uniform. Hence, it can be asserted that the implementation of a perforated plate situated on the front of the oven has substantially enhanced the uniformity of temperature and fluid velocity.

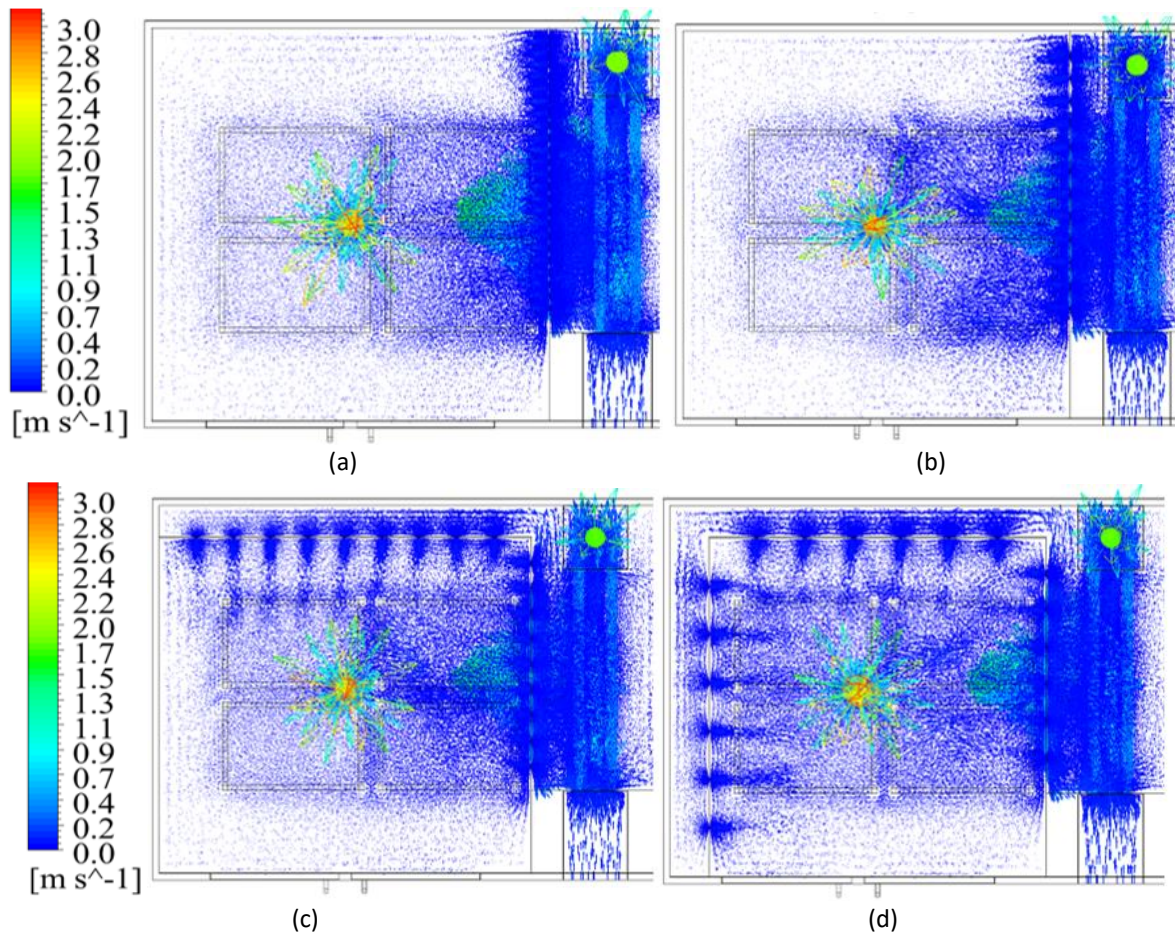


**Fig. 13.** Airflow pattern of the oven with (a) original geometry, (b) 1st geometry, (c) 2nd geometry, and (d) 3rd geometry viewed from the top side of the oven

#### 4. Conclusions

The purpose of this study is to determine the effect of perforated plate geometry on thermofluid characteristics, which include air temperature distribution, air velocity, airflow pattern, and air pressure in the briquette drying oven. CFD simulations were conducted on both the original oven and the modified oven, which had three different geometries. The findings obtained from this investigation are as follows:

- i. The average temperatures in the original, first geometry, second geometry, and third geometry ovens are 74.093°C, 79.173°C, 79.562°C, and 80.869°C, respectively. An increase of 6.86%, 7.38%, and 9.15% was observed in the average temperature of the ovens with the first, second, and third geometries, correspondingly, due to the utilization of perforated plates. The temperature differences between the original, first, second, and third geometry ovens are 22.376°C, 28.757°C, 23.030°C, and 20.714°C, respectively.
- ii. The average air velocity in the original, first, second, and third oven geometry is 0.0326 m/s, 0.1063 m/s, 0.1095 m/s, and 0.1733 m/s, respectively. The use of perforated plates enhances the average air velocity in ovens with the first, second, and third geometries by 226.04%, 235.77%, and 431.60%, respectively.
- iii. The average air pressure in the original oven was 2267.05 Pa. The use of perforated plates causes a decrease in the average air pressure in the oven. In ovens with the first, second, and

third geometries, the resulting air pressure is 2016.47 Pa, 2071.64 Pa, and 2025.40 Pa. The average reduction in air pressure in ovens with the first, second, and third geometries is 11.05%, 8.62%, and 10.66%, respectively.

- iv. The airflow pattern in the first and original ovens was concentrated on the right side of the oven. The airflow pattern is more uniform in the oven utilizing the second geometry compared to the ovens utilizing the first and original geometries. This occurs due to the utilization of perforated plates situated on the rear and right sides of the oven. Compared to other oven models, the airflow pattern in the third geometry oven is superior.
- v. This occurs due to the airflow passing through the perforated plates on the left, right, and posterior surfaces. As a result, air circulation becomes more uniform.
- vi. Perforated plates enhance the oven's average air temperature and average air velocity. This leads to enhancements in the evaporation of water vapor, the movement of moisture, and the effectiveness of drying by increasing the transfer of mass and the contact surface area between the air and the substance. Therefore, the process of drying can be expedited. Utilizing perforated plates results in a reduction in the average air pressure within the oven. This results in a reduction in air humidity. This can expedite the drying process, as air with low humidity has a diminished capacity to retain water vapor. Therefore, low humidity air can accelerate the process of removing water from the dried material.
- vii. The use of perforated plates on the right, back, and left sides in an oven with the third geometry is the best geometry produced in this research. This happens because this oven produces the most even airflow pattern in the oven compared to other geometries. In addition, the oven with the third geometry has the highest average temperature and average air velocity, with a lower average air pressure compared to the other geometries.
- viii. The scope of this research is limited to three different configurations of perforated plates used in briquette drying ovens. Therefore, in future investigations, further variations are needed, including adjustments to the geometry of the combustion furnace, tray, inlet air velocity, and inlet air temperature. Furthermore, it is essential to examine the effects of oven geometry on drying time and air density. This is a critical stage in obtaining a briquette drying oven that is more effective and efficient, thereby contributing to future fuel and production cost savings.

### Acknowledgement

The authors would like to thank Universitas Negeri Semarang (UNNES) for allocating funds under the Penelitian Terapan Kepakaran Scheme in 2024 with contract number 244.26.2/UN37/PPK.10/2024.

### References

- [1] Wu, Shunyan, Shouyu Zhang, Caiwei Wang, Chen Mu, and Xiaohe Huang. "High-strength charcoal briquette preparation from hydrothermal pretreated biomass wastes." *Fuel Processing Technology* 171 (2018): 293-300. <https://doi.org/10.1016/j.fuproc.2017.11.025>.
- [2] Efiyanti, L., S. Darmawan, N. A. Saputra, H. S. Wibisono, D. Hendra, and G. Pari. "Quality evaluation of coconut shell activated carbon and its application as precursor for citronellal-scented aromatic briquette." *Rasayan Journal of Chemistry* 15, no. 3 (2022): 1608-1618. <https://doi.org/10.31788/RJC.2022.1536799>.
- [3] Bayu, Abreham Bekele, T. A. Amibo, and D. A. Akuma. "Conversion of degradable municipal solid waste into fuel briquette: case of Jimma city municipal solid waste." *Iranica Journal of Energy & Environment* 11, no. 2 (2020): 122-129. <https://doi.org/10.5829/ijee.2020.11.02.05>.
- [4] Anis, Samsudin, Deni Fajar Fitriyana, Aldias Bahatmaka, Muhammad Choirul Anwar, Arsyad Zanadin Ramadhan, Fajar Chairul Anam, Raffanel Adi Permana, Ahmad Jazilussurur Hakim, Natalino Fonseca Da

- Silva Guterres, and Mateus De Sousa Da Silva. "Effect of Adhesive Type on the Quality of Coconut Shell Charcoal Briquettes Prepared by the Screw Extruder Machine." *Journal of Renewable Materials* 12, no. 2 (2024).
- [5] Fitriyana, D. F., F. W. Nugraha, M. B. Laroybafih, R. Ismail, A. P. Bayuseno, R. C. Muhamadin, M. B. Ramadan, A. RA Qudus, and J. P. Siregar. "The effect of hydroxyapatite concentration on the mechanical properties and degradation rate of biocomposite for biomedical applications." In *IOP Conference Series: Earth and Environmental Science*, vol. 969, no. 1, p. 012045. IOP Publishing, 2022.
- [6] Fitriyana, Deni Fajar, Agustinus Purna Irawan, Aldias Bahatmaka, Rifky Ismail, Athanasius Priharyoto, Rilo Chandra Muhamadin, Tezara Cionita, Januar Parlaungan Siregar, and Emilianus Jehadus. 2023. "The effect of temperature on the hydrothermal synthesis of carbonated apatite from calcium carbonate obtained from green mussels shells." *ARPN Journal of Engineering and Applied Sciences* 18 (11): 1215–1224.
- [7] Azmi, Mohamad Zaharan, Ibni Hajar Rukunudin, Hirun Azaman Ismail, and Aimi Athirah Aznan. "Specific Energy Consumption and Drying Efficiency Analysis of Commercial Mixed-Flow Batch Type Seed Drying System." *Journal of Advanced Research in Fluid Mechanics and Thermal Sciences* 55, no. 1 (2019): 39-50.
- [8] Misha, Suhaimi, Sohif Mat, Mohd Hafidz Ruslan, Elias Salleh, and Kamaruzzaman Sopian. "A Study of Drying Uniformity in a New Design of Tray Dryer." *Journal of Advanced Research in Fluid Mechanics and Thermal Sciences* 52, no. 2 (2018): 129-138.
- [9] Schueftan, Alejandra, Jorge Sommerhoff, and Alejandro D. González. "Firewood demand and energy policy in south-central Chile." *Energy for Sustainable Development* 33 (2016): 26-35. <https://doi.org/https://doi.org/10.1016/j.esd.2016.04.004>.
- [10] Ngusale, George K., Yonghao Luo, and Jeremiah K. Kiplagat. "Briquette making in Kenya: Nairobi and peri-urban areas." *Renewable and Sustainable Energy Reviews* 40 (2014): 749-759. <https://doi.org/https://doi.org/10.1016/j.rser.2014.07.206>.
- [11] Prasetyadi, Andreas, and Wibowo Kusbandono. "High Performance Oven for Coconut Shell Charcoal Briquetting." In *4th Borobudur International Symposium on Science and Technology 2022 (BIS-STE 2022)*, pp. 101-110. Atlantis Press, 2023. [https://doi.org/10.2991/978-94-6463-284-2\\_13](https://doi.org/10.2991/978-94-6463-284-2_13).
- [12] Díaz-Ovalle, Christian O., Ricardo Martínez-Zamora, Guillermo González-Alatorre, Lucero Rosales-Marines, and Raúl Lesso-Arroyo. "An approach to reduce the pre-heating time in a convection oven via CFD simulation." *Food and bioproducts processing* 102 (2017): 98-106. <https://doi.org/https://doi.org/10.1016/j.fbp.2016.12.009>.
- [13] Ngo, Thi-Thao, Chi-Chang Wang, Hsiao-Hui Wu, and Van-The Than. "Improving temperature uniformity of glass panels in TFT-LCD oven based on perforated plates." *Thermal Science and Engineering Progress* 19 (2020): 100592. <https://doi.org/https://doi.org/10.1016/j.tsep.2020.100592>.
- [14] Khovanskyi, Serhii, Ivan Pavlenko, Jan Pitel, Jana Mizakova, Marek Ochowiak, and Irina Grechka. "Solving the coupled aerodynamic and thermal problem for modeling the air distribution devices with perforated plates." *Energies* 12, no. 18 (2019): 3488. <https://doi.org/10.3390/en12183488>.
- [15] Marković, Zoran J., Mili Erić, Rastko Jovanović, and Ivan Lazović. "Numerical simulation of the gas flow through the rectangular channel with perforated plate." *Thermal Science* 00 (2023): 89-89. <https://doi.org/10.2298/TSCI220426089M>.
- [16] Li, Hao, Zhi Jun Zou, and Fei Wang. "The effect of orifice plate on flow field and thermal environment in oven box." *Applied Mechanics and Materials* 713 (2015): 47-50. <https://doi.org/10.4028/www.scientific.net/amm.713-715.47>.
- [17] Dhanuskar, Vaibhav C, and Pramod R Pachghare. "Modeling and Analysis of Temperature Distribution in the Industrial Gas Fired Powder Coating Oven Using Computational Fluid Dynamic (CFD)." *International Journal of Innovative Research in Science, Engineering and Technology* 6, no. 6 (2017): 10503–9. <https://doi.org/10.15680/IJRSET.2017.0606052>.
- [18] Tomić, Mladen A., Sadoon K. Ayed, Žana Ž. Stevanović, Petar S. Đekić, Predrag M. Živković, and Mića V. Vukić. "Perforated plate convective heat transfer analysis." *International Journal of Thermal Sciences* 124 (2018): 300-306. <https://doi.org/https://doi.org/10.1016/j.ijthermalsci.2017.10.021>.



- [19] Li, Quan, Xuxu Sun, Xing Wang, Zhi Zhang, Shouxiang Lu, and Changjian Wang. "Geometric influence of perforated plate on premixed hydrogen-air flame propagation." *International Journal of Hydrogen Energy* 43, no. 46 (2018): 21572-21581. <https://doi.org/https://doi.org/10.1016/j.ijhydene.2018.09.138>.
- [20] Raju, L. Ratna, S. Sunil Kumar, K. Chowdhury, and T. K. Nandi. "Heat transfer and flow friction correlations for perforated plate matrix heat exchangers." In *IOP Conference Series: Materials Science and Engineering*, vol. 171, no. 1, p. 012085. IOP Publishing, 2017. <https://doi.org/10.1088/1742-6596/755/1/011001>.
- [21] Forrester, Alexander IJ, Neil W. Bressloff, and Andy J. Keane. "Optimization using surrogate models and partially converged computational fluid dynamics simulations." *Proceedings of the Royal Society A: Mathematical, Physical and Engineering Sciences* 462, no. 2071 (2006): 2177-2204. <https://doi.org/10.1098/rspa.2006.1679>.
- [22] Einarsrud, Kristian Etienne, Varun Loomba, and Jan Erik Olsen. "Applied Computational Fluid Dynamics (CFD)." *Processes* 11, no. 2 (2023): 461. <https://doi.org/10.3390/pr11020461>.
- [23] Araújo, Morgana de Vasconcellos, Antonildo Santos Pereira, Jéssica Lacerda de Oliveira, Vanderson Alves Agra Brandão, Francisco de Assis Brasileiro Filho, Rodrigo Moura da Silva, and Antonio Gilson Barbosa de Lima. "Industrial ceramic brick drying in oven by CFD." *Materials* 12, no. 10 (2019): 1612. <https://doi.org/10.3390/ma12101612>.
- [24] Hudaningsih, Nurul, Iksan Adiasa, Azzam Safaroh Saefullah, and Sopyan Ali Rohman. "Optimization of Thermal Distribution in Masin Fermenters Using Computational Fluid Dynamic Method with Ansys Software." <https://doi.org/10.46254/ap03.20220091>.
- [25] Edirisinghe, Dylan S., Ho-Seong Yang, S. D. G. S. P. Gunawardane, and Young-Ho Lee. "Enhancing the performance of gravitational water vortex turbine by flow simulation analysis." *Renewable Energy* 194 (2022): 163-180. <https://doi.org/https://doi.org/10.1016/j.renene.2022.05.053>.
- [26] Park, Seong Hyun, Yang Ho Kim, Young Soo Kim, Yong Gap Park, and Man Yeong Ha. "Numerical study on the effect of different hole locations in the fan case on the thermal performance inside a gas oven range." *Applied Thermal Engineering* 137 (2018): 123-133. <https://doi.org/https://doi.org/10.1016/j.applthermaleng.2018.03.087>.
- [27] Seeni, Aravind, Parvathy Rajendran, and Hussin Mamat. "A CFD mesh independent solution technique for low Reynolds number propeller." (2021).
- [28] Horuz, Erhan, Hüseyin Bozkurt, Haluk Karataş, and Medeni Maskan. "Drying kinetics of apricot halves in a microwave-hot air hybrid oven." *Heat and Mass transfer* 53 (2017): 2117-2127. <https://doi.org/10.1007/s00231-017-1973-z>.
- [29] Setyadi, P., N. G. Yoga, R. Anggrainy, O. F. Hidayat, and Y. F. N. Syamsy. "Energy Saving on Spray Drying Process by Modifying the Hot Air Flow." In *Journal of Physics: Conference Series*, vol. 2377, no. 1, p. 012060. IOP Publishing, 2022. <https://doi.org/10.1088/1742-6596/2377/1/012060>.
- [30] Inyang, Uwem Ekwere, Innocent Oseribho Oboh, and Benjamin Reuben Etuk. "Kinetic models for drying techniques—food materials." *Advances in Chemical Engineering and Science* 8, no. 2 (2018): 27-48. <https://doi.org/10.4236/aces.2018.82003>.
- [31] Putra, Raka Noveriyan, and Tri Ayodha Ajiwiguna. "Influence of air temperature and velocity for drying process." *Procedia engineering* 170 (2017): 516-519. <https://doi.org/10.1016/j.proeng.2017.03.082>.
- [32] Smolka, Jacek, Zbigniew Bulinski, and Andrzej J. Nowak. "The experimental validation of a CFD model for a heating oven with natural air circulation." *Applied thermal engineering* 54, no. 2 (2013): 387-398. <https://doi.org/https://doi.org/10.1016/j.applthermaleng.2013.02.014>.
- [33] Quan, Mengfan, Yu Zhou, Lei Jia, Yi Wang, Xiaoni Yang, Yuxin Fang, and Zhixiang Cao. "The realization of parallel airflow after flow rectification by the perforated plate under complex inflows." *Journal of Building Engineering* 76 (2023): 107120. <https://doi.org/https://doi.org/10.1016/j.jobe.2023.107120>.
- [34] Wang, Danyang, Chenghua Li, Benhua Zhang, and Ling Tong. "Exploring the Effect Rules of Paddy Drying on a Deep Fixed-Bed." In *Computer and Computing Technologies in Agriculture IX: 9th IFIP WG 5.14 International Conference, CCTA 2015, Beijing, China, September 27-30, 2015, Revised Selected Papers*,

- Part 1 9, pp. 473-484. Springer International Publishing, 2016. [https://doi.org/10.1007/978-3-319-48357-3\\_45](https://doi.org/10.1007/978-3-319-48357-3_45).
- [35] Pereira, Nádia R., Antonio Marsaioli Jr, and Lília M. Ahrné. "Effect of microwave power, air velocity and temperature on the final drying of osmotically dehydrated bananas." *Journal of Food Engineering* 81, no. 1 (2007): 79-87. <https://doi.org/https://doi.org/10.1016/j.jfoodeng.2006.09.025>.
- [36] Husin, Husni, Asri Gani, and Rizalman Mamat. "Modification of perforated plate in fluidized-bed combustor chamber through computational fluid dynamics simulation." *Results in Engineering* 19 (2023): 101246. <https://doi.org/https://doi.org/10.1016/j.rineng.2023.101246>.
- [37] Wakid, Muhkamad, Aan Yudianto, and Agus Widyianto. "Numerical Modelling and Analysis of Externally Blown Heated Pipes Applicable for Furnace." *Journal of Advanced Research in Fluid Mechanics and Thermal Sciences* 100, no. 1 (2022): 30-43. <https://doi.org/10.37934/arfmts.100.1.3043>.
- [38] Balzarini, Maria Florencia, Maria Agustina Reinheimer, Maria Cristina Ciappini, and Nicolas Jose Scenna. "Comparative study of hot air and vacuum drying on the drying kinetics and physicochemical properties of chicory roots." *Journal of food science and technology* 55 (2018): 4067-4078. <https://doi.org/10.1007/s13197-018-3333-5>.
- [39] Salehi, Fakhreddin, and Mahdi Kashaninejad. "Modeling of moisture loss kinetics and color changes in the surface of lemon slice during the combined infrared-vacuum drying." *Information processing in Agriculture* 5, no. 4 (2018): 516-523. <https://doi.org/https://doi.org/10.1016/j.inpa.2018.05.006>.
- [40] Li, Gongfa, Wei Miao, Guozhang Jiang, Yinfeng Fang, Zhaojie Ju, and Honghai Liu. "Intelligent control model and its simulation of flue temperature in coke oven." *Discrete and continuous dynamical systems-series s* 8, no. 6 (2015): 1223-1237. <https://doi.org/10.3934/dcdss.2015.8.1223>.
- [41] Elfiana, E., Usman Usman, Muhammad Sami, Ridwan Ridwan, Syarifah Keumala Intan, Cut Aja Rahmawati, Salmiyah Salmiyah, and Pardi Pardi. "Desiminasi Oven Drying Vacuum (ODV) Untuk Pengeringan Rempah Bandrek Siap Saji Di Desa Kumbang Kecamatan Syamtalira Aron Kabupaten Aceh Utara." In *Prosiding Seminar Nasional Politeknik Negeri Lhokseumawe*, vol. 5, no. 1, pp. 147-154. 2021.
- [42] Zi, Pingyang, Youliang Chen, Jiangang Hao, and Daxing Xie. "Analysis of Influence of Atmospheric Parameter Fluctuation on Condenser Pressure." In *IOP Conference Series: Materials Science and Engineering*, vol. 721, no. 1, p. 012063. IOP Publishing, 2020. <https://doi.org/10.1088/1757-899X/721/1/012063>.
- [43] Matbabayevich, Matbabayev Mahmud. "Temperature and Humidity Parameters of the Air Environment in Industrial Premises." *International Journal on Orange Technologies* 3, no. 6 (2023): 89-94.
- [44] N.Susanto. "The Influence of Air Pressure on the Rate of Mass Change in the Drying Process Using the Low Temperature Drying Method." UNNES, Semarang, Indonesia., 2011.
- [45] Verma, Sunil, A. B. Usenov, D. U. Sobirova, S. A. Sultonova, and J. E. Safarov. "Mathematical description of the drying process of mulberry leaves." In *IOP Conference Series: Earth and Environmental Science*, vol. 1112, no. 1, p. 012012. IOP Publishing, 2022. <https://doi.org/10.1088/1755-1315/1112/1/012012>.
- [46] Ali, Majid Khan Majahar, Ahmad Fudholi, M. S. Muthuvalu, Jumat Sulaiman, and Suhaimi Md Yasir. "Implications of drying temperature and humidity on the drying kinetics of seaweed." In *AIP Conference Proceedings*, vol. 1905, no. 1. AIP Publishing, 2017. <https://doi.org/10.1063/1.5012223>.
- [47] Doran, Pauline M. "Chapter 11 - Unit Operations." In *Bioprocess Engineering Principles (Second Edition)*, edited by Pauline M B T - *Bioprocess Engineering Principles (Second Edition)* Doran, 445-595. London: Academic Press, 2013. <https://doi.org/https://doi.org/10.1016/B978-0-12-220851-5.00011-3>.
- [48] Pask, Frederick, Peter Lake, Aidong Yang, Hella Tokos, and Jhuma Sadhukhan. "Industrial oven improvement for energy reduction and enhanced process performance." *Clean Technologies and Environmental Policy* 19 (2017): 215-224. <https://doi.org/10.1007/s10098-016-1206-z>.
- [49] Luo, Xuan, Guozhong Cui, and Fulong Le. "Heat distribution mathematical model and numerical simulation of an electric oven." In *Proceedings of the 33rd Chinese Control Conference*, pp. 6445-6448. IEEE, 2014. <https://doi.org/10.1109/ChiCC.2014.6896052>